Improvements in Adaptive Mesh Refinement and Multilevel Methods in High-Frequency Electromagnetics

Istvan Bardi Gaunghua Peng Zoltan J. Cendes
Ansoft Corporation, Pittsburgh, PA
Email: zol@ansoft.com

ABSTRACT

During the past twelve years, great improvements in finite element solution algorithms have been made. In 1990, a simple coax to waveguide adapter took sixteen hours to solve for a single frequency point on a Sun II computer; today the same part is solved for a fast sweep of 10 or more frequency points on a Pentium IV computer in 6 seconds. This is speed improvement of over 90,000 times. This paper shows the role that better mesh refinement algorithms, better error estimation criteria, multifrontal matrix solution procedures, hierarchical basis functions, and multilevel methods have played in this speed-up.

INTRODUCTION

HFSS was the first commercial software package in any field to employ adaptive mesh refinement [1]. Developed in 1990 by Ansoft Corporation and marketed for the first six years by the Hewlett-Packard Corporation, HFSS has from the beginning had the ability to automatically refine the mesh in regions of high error and to display the convergence of the results with respect to adaptive solution passes.

During the past twelve years, great improvements in the adaptive mesh refinement process and in the use of multifrontal multilevel methods have been made. Back in 1990, a simple coax to waveguide adapter (HP Part # R282A) took sixteen hours to solve on a Sun II computer; today the same part is solved in HFSS on a Pentium IV computer in 6 seconds. This is speed improvement of over 10,000 times. While part of this speed-up is due to improvements in computer hardware execution speed, an even greater part is due to improvements in the simulation algorithms. In particular, better mesh refinement algorithms, better error estimation criteria, multifrontal matrix solution procedures, hierarchical basis functions, and multilevel methods have all contributed to more than doubling the speed of the solution process in HFSS every year for twelve years.

Through the years, a number of adaptive refinement criteria have been used. The early code relied on complementary error bounds [2] to determine local errors in the solution. While highly accurate and reliable, the first complementary error bounds required the solution of two field problems and thus were less efficient than one-sided error indicators. One-sided error indicators include residual methods, local Dirichlet and Neumann approximations, Green's function methods, and error charge/error current methods [3]. Convergence to the solution has been more rapid with each successive error indicator; many problems now solve to a given accuracy using one or two orders of magnitude fewer elements than was possible with the earlier code.

A second factor in speeding up the finite element solution process has been the development of better matrix solution algorithms and better approximation functions. The original code in 1990 used a direct sparse matrix solution algorithm and $H^1(curl)$ finite elements [4]. Since then great improvements in both matrix solution algorithms and in finite element basis functions have been made. The first of these improvements was the use of multifrontal algorithms. Multifrontal algorithms exploit computer architecture and subblocks within the sparse finite element matrix to accelerate the matrix solution process. With multifrontal algorithms, even a million unknown $H^1(curl)$ element matrix problem can be solved on a PC in less than 5 minutes. As a larger example, a 12-way power divider involving 3,813,428 unknowns using $H^1(curl)$ elements requires 1 hour 33 minutes and 42 seconds for matrix solution on a Sun workstation in the current shipping code.

The most recent work employs a combination of multifrontal direct solution and iterative multilevel solutions. Conventional multilevel methods employ a nested grid based on a multilevel of grids. In our work, the multilevel algorithm employs a single grid but a multilevel of hierarchical basis functions. We begin with the $H^0(curl)$ element and factor the system matrix using the multifrontal solver. The order of the basis functions is then increased and the $H^0(curl)$ results are used in Schur decomposition to obtain an approximate inverse of part of the $H^1(curl)$ matrix. This approximate inverse is used as a preconditioner for the conjugate gradient method. The process can be repeated to achieve higher orders. Of course, the convergence of the above procedure depends on the basis functions used in the approximation. We have developed procedures to generate an optimal set of hierarchical basis functions for convergence with the conjugate gradient algorithm [5].

This paper includes examples of large industrial problems solved using HFSS. The speed improvement due to better error indicators and due to better matrix solution algorithms will be presented.

MESH GENERATION

Adaptive mesh generation is closely linked to the ability to create unstructured meshes. Unstructured meshes allow additional vertices to be placed anywhere in the solution region and thereby concentrate elements where they are most required. An excellent way to form unstructured meshes is by means of Delaunay tessellation, a procedure introduced in finite element analysis in [2]. The technology developed in these references and used in HFSS begins by making an initial, unstructured, minimal mesh given the problem geometry. This mesh is then refined by using a procedure is called "Material Dependent Lambda Refinement" to create a wavelength-based initial mesh density. The third step is to solve the problem on the existing mesh, estimate the error in each element in the mesh, and refine those elements having the highest errors.

The reason for Material Dependent Lambda Refinement is that a minimal mesh density is required in microwave applications to support wave propagation. The number of tetrahedra required per wavelength depends on the degree of the elements; in the case of $H_1(curl)$ elements, this number is 4. The mesh generation strategy in HFSS is therefore to begin by creating a nearly uniform mesh for each object having a different material.

To demonstrate the behavior of the Material Dependent Lambda Refinement, two examples are presented. The first example is the calculation of the Radar Cross Section of

a dielectric sphere. PMLs are used to terminate the domain and two adaptive refinement procedures are compared. Figure 1 shows the comparison of the convergence behavior of the adaptive mesh refinement without and with material dependent lambda refinement. It can be seen that material dependent lambda refinement requires no significant refinement to obtain convergence. Figure 2 shows a comparison of the calculated and the analytical values of the normalized bistatic radar cross-section. The agreement is excellent. Material dependent lambda refinement required less CPU time, since it converged after the first step, while full adaptive refinement required 4 steps. The second example is a cavity resonator inhomogeneously filled with dielectric materials. Figure 3 shows that the solution practically converged after the first refinement.

Thus if the field pattern is nearly homogeneous, as in the above cases, the minimal mesh is sufficient and little additional refinement is necessary. If the field pattern is inhomogeneous, such as problems involving corner singularities, then the local error in the minimal mesh solution is estimated and elements having large errors are refined.

There are two cases where material dependent lambda refinement results in unnecessarily large meshes. One case is where the propagation is unidirectional such as in microstrip lines and dielectric resonators. The electromagnetic field decays strongly in certain directions and the mesh can be reduced in these directions to avoid creating unnecessarily large meshes. The other case is wh
materials. Electromagnetic waves decay rapidly in t
to refine high-loss objects near the surface. Mate
disabled in these objects.

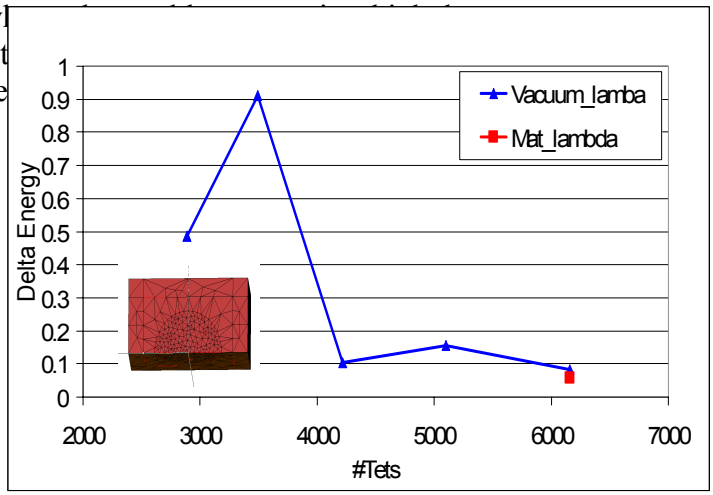

Figure 1: Convergence behavior of a dielectric sphere in an incident wave

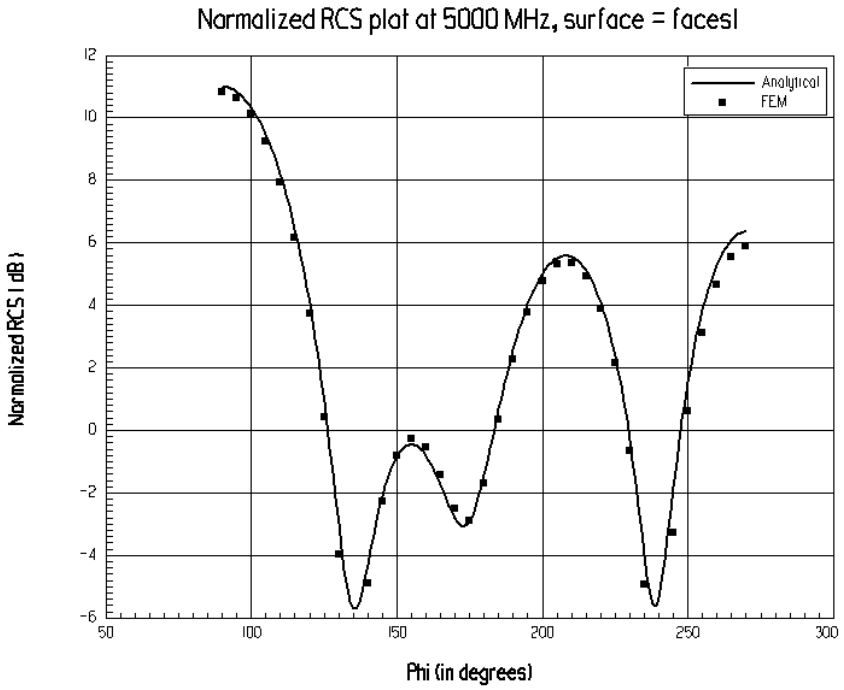

Figure 2: Calculated and analytical values of the bistatic RCS of a dielectric sphere R = 0.03 m, f = 5GHz, $\varepsilon_r = 10$, $\lambda/D=1$

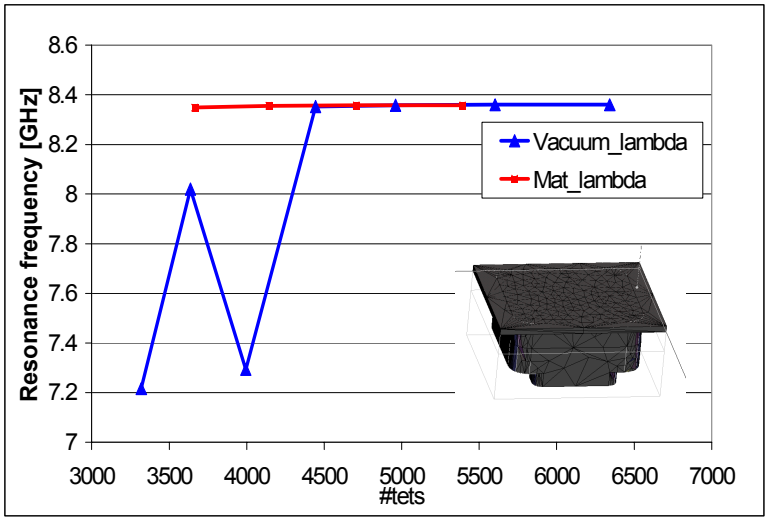

Figure 3: Convergence behavior of an inhomogeneously filled cavity resonator

ERROR ESTIMATORS

Central to the mathematical theory of the finite element method is the convergence of the method to a unique solution as the finite element mesh and the basis functions finite element are refined. This refinement is usually discussed in mathematical texts in terms of uniformly refining the mesh – called h refinement – or in terms of uniformly increasing the polynomial order of the approximation functions – called p-refinement. A better approach is to refine the mesh non-uniformly by concentrating elements where

they are needed most, or to increase the polynomial order non-uniformly by concentrating basis functions were they are needed most. The first of these approaches is called adaptive mesh refinement; the second adaptive function refinement. Both strategies provide dramatic improvements in the rate of convergence.

The key to success with either adaptive mesh refinement or adaptive function refinement is to use an effective error estimation criterion. The general strategy is to solve the problem first using a coarse, low order basis function mesh and then to estimate the error in each element on this coarse mesh. Wherever the error is highest, the mesh and/or the basis functions are refined. The process is repeated iteratively until the error is reduced to a predefined level.

HFSS has two different built in procedures for estimating errors:

1. Residual error calculation
2. Complementary variational principles

Residual error calculation is an extension of the local approximation procedure introduced by Bank [6]. In Bank's approach, a small local finite element problem with either Dirichlet or Neuman boundary conditions is solved for each element in the mesh. Since the local problem is small – on the order of 3 to 15 separate unknowns per element – the computational cost of this method is linear with problem size. However, an extension of the method by Shenton and Cendes [3] shows how to compute the local errors without performing these small matrix solutions.

To describe the Shenton-Cendes error estimation procedure, consider the vector wave equation in terms of the electric field vector

$$curl[\nu_r]curl\mathbf{E} - k_0^2[\varepsilon_r]\mathbf{E} = -jw\mathrm{J} \tag{1}$$

with boundary conditions

$$\mathbf{n}\times\mathbf{E} = \mathbf{n}\times\mathbf{E}_{t0} \qquad \text{on } \Gamma_E \text{ (Ports)} \tag{2}$$

$$\mathbf{n}\times[\nu_r]\nabla\times\mathbf{E} = \begin{cases} -j\omega\mu_0\mathbf{n}\times\mathbf{H}_{t0} \\ -j\omega\mu_0 Y_0\mathbf{n}\times\mathbf{n}\times\mathbf{E} \end{cases} \qquad \text{on } \Gamma_H \text{ (Impedance and ABC)} \tag{3}$$

Here $[\varepsilon_{rc}]$ and $[\mu_{rc}]$ are the complex relative permittivity and permeability tensors, respectively, $[\nu_{rc}]$ is the inverse of $[\mu_{rc}]$, Y_0 is the complex surface admittance defined on Γ_H and **J** is zero in source-free regions. Associated with (1) is the functional

$$F = \int_\Omega (\nabla\times\mathbf{E}^* \bullet [\nu_{rc}]\mathbf{E} - k_0^2\mathbf{E}^* \bullet [\varepsilon_{rc}]\mathbf{E})d\Omega + \int_{\Gamma_H} (\mathbf{n}\times\mathbf{E}^*) \bullet (j\omega\mu_0(\mathbf{n}\times\mathbf{H_{t0}} + Y_0\mathbf{n}\times\mathbf{E}))d\Gamma \tag{4}$$

The discretization of (1) using tangential vector finite elements by either Galerkin's method or by extremizing the functional F leads to the algebraic equation [7]

$$(\mathbf{A} - k_0^2\mathbf{B})\mathbf{x} = \mathbf{b} \tag{5}$$

where

$$A_{i,j} = \int_\Omega \nabla\times\mathbf{N}_i \bullet [\nu_{rc}]\nabla\times\mathbf{N}_j d\Omega \tag{6}$$

$$B_{i,j} = \int_{\Omega} \mathbf{N_i} \bullet [\varepsilon_{rc}] \mathbf{N_j} d\Omega + j\omega\mu_0 \int_{\Gamma_H} Y_0 (\mathbf{n} \times \mathbf{N_i}) \bullet (\mathbf{n} \times \mathbf{N_j}) d\Gamma \tag{7}$$

$$b_i = -j\omega\mu_0 \int_{\Gamma_H} \mathbf{n} \times \mathbf{N}_i \bullet (\mathbf{n} \times \mathbf{H_{t0}}) d\Gamma \tag{7}$$

Here $\mathbf{N}_i$ and $\mathbf{N}_i$ are vector shape functions and the column matrix $\boldsymbol{x}$ contains the coefficients of the interpolation of $\boldsymbol{E}$**.** Ansoft HFSS uses *H_0(curl)*, *H_1(curl)* … *H_p(curl)* vector finite elements in tetrahedra [8].

Solving (5) provides an approximate solution to (1). Let us call the exact solution of (1) $\mathbf{E}^{\text{exact}}$ and the approximate solution of (5) $\mathbf{E}^{\text{approx}}$. Since the approximate solution is not exact except for trivial problems, using $\mathbf{E}^{\text{approx}}$ in (1) provides a residual

$$r = curl[\nu_r] curl \mathbf{E} approx - k_0^2 [\varepsilon_r] \mathbf{E} approx + jw\mathbf{J} \tag{8}$$

The error in the solution is

$$e = \mathbf{E}\text{exact} - \text{Eapprox} \tag{9}$$

Inserting the error into the left-hand-side of (1) yields

$$\begin{aligned} &curl[\nu_r] curle - k_0^2 [\varepsilon_r] e \\ &= curl[\nu_r] curl \mathbf{E}\text{exact} - k_0^2 [\varepsilon_r] \mathbf{E}\text{exact} - curl[\nu_r] curl \mathbf{E} approx + k_0^2 [\varepsilon_r] \mathbf{E} approx \end{aligned} \tag{10}$$

The first two terms in (10) yield –jwJ; the second two terms yield r+jwJ. Thus (10) becomes

$$curl[\nu_r] curle - k_0^2 [\varepsilon_r] e = r \tag{11}$$

It follows that the error may be computed by solving the vector wave equation taking the forcing function to be the residual. Comparing (1) and (11), we see that the residual r may be thought of as an "error current" – i.e., as a current component on the right-hand-side of the vector wave equation that generates the error in the field. To estimate e, we multiply (11) through by the shape function $\mathbf{N}_i$, integrate and apply a vector identity. The result is

$$\int_{\Omega} (\nabla \times N \bullet [\nu_{rc}] e - k_0^2 N \bullet [\varepsilon_{rc}] e) d\Omega + \int_{\Gamma_H} N \bullet (j\omega\mu_0 (\mathbf{n} \times e)) d\Gamma = \int_{\Omega} (N \bullet r) d\Omega \tag{12}$$

Examining the continuity conditions at inter-element boundaries shows that the boundary term in (12) is zero and that the magnitude of e may be estimated by approximating e by the finite element basis functions [9].

The other approach for estimating errors in HFSS is to use complementary variational principles. Complementary variational principles make it is possible to determine rigorous upper and lower bounds for the global error in an approximate solution [10]. Cendes, Shenton and Shahnasser [2] employed this idea in 1983 to provide local finite element error estimates with Delaunay meshes for electrostatics and magnetostatics problems. The procedure was extended to wave propagation problems by Lee, Sun and

Cendes [4]. An outline of the procedure is as follows: The reaction of a field a on a source b is

$$\langle a \mid b \rangle = \int_{\Omega} (\mathbf{E}^a \bullet J^b - H^a \bullet M^b) d\Omega \tag{13}$$

The sources J^b and M^b are the residuals

$$J^b = \nabla \times H^b - j\omega\varepsilon\mathbf{E}^b \tag{14}$$

$$M^b = -\nabla \times \mathbf{E}^b - j\omega\mu H^b \tag{15}$$

The reaction of the exact solution is zero because for the exact solution J^b and M^b are zero. Thus we let a=b and (13) reduces to

$$\langle a \mid a \rangle = \int_{\Omega} (\mathbf{E}^a \bullet J^a - H^a \bullet M^a) d\Omega = 0 \tag{16}$$

(16) provides the complementary error estimation procedure in HFSS. The functional (4), which is minimized during the solution, is proportional to the difference in magnetic and electric energies [11]. The distribution of the local functional - which is considered to characterize the error – is not uniform. [12] states that the best mesh is on which the error distribution is uniform. It follows that the mesh should be refined where the local value of the functional is high. The complementary variation principle based error estimator is called as classic error estimator in HFSS.

ADAPTIVE MESH REFINEMENT

The crucial question for both error estimators is how well they cope with singularities in the electromagnetic field. Most microwave structures contain edges and corners. The accuracy of the solution depends on approximating the singularities well. In the following, we present examples that show the importance of the treatment of the singularity.

The first example is a floating dipole in a parallel plate waveguide (Fig. 5). Figure 6 shows the excellent convergence of the classic method. The electric field has singularities at the corners of the floating dipole, while the singularity of the magnetic field is along the edges of the dipole. The order of the singularity of the electric field is higher than that of the magnetic field. It can be seen in Figure 7 that the mesh copes with this problem. The mesh is denser at the corners and less dense along the edges, though it is dense enough compared to other regions.

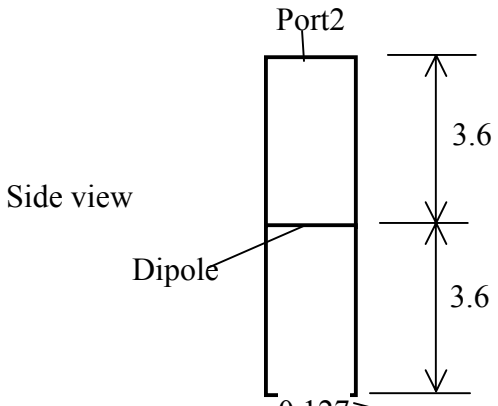

Figure 5: The layout of a floating dipole in a parallel plate waveguide. The dimensions are in cm; f = 10.5 GHz

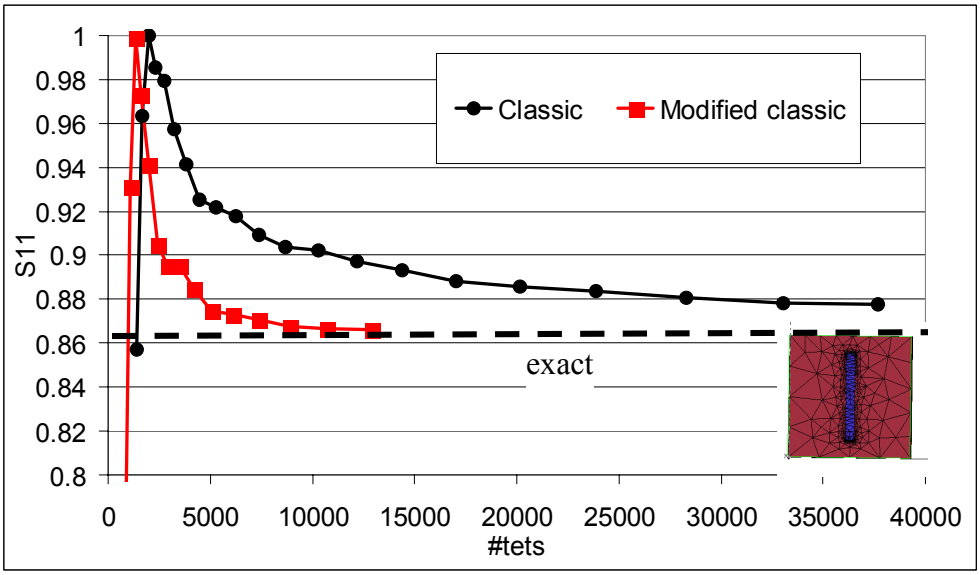

Figure 6: Convergence of the classic and the modified classic error estimator in the case of a floating dipole.

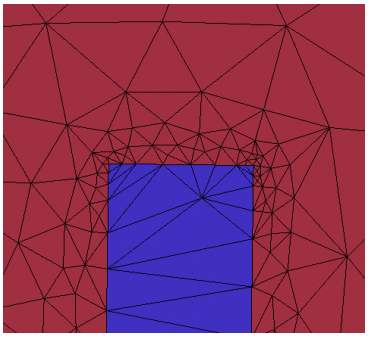

Figure 7: Mesh in the plane of the floating dipole.

The second example is a slot in a parallel plate waveguide. The geometry is the same as it was the previous example, but the PEC and PMC boundary conditions have been exchanged. This is the dual problem of the floating dipole. Figure 8 shows good convergence again.

The next example is a Low Pass Filter as it can be seen in Fig. 9. The structure has more singularities. The classic method is superior to the residual one as it can be seen from the convergence behavior.

The next example is a half wavelength dipole antenna. The antenna is excited by a gap source. Since the diameter of the wire of the antenna is very small and it is cylindrical, the simulation of the singularity plays an important role in the result. Fig. 10 shows again the excellent convergence of the classic method. The directivity pattern of the antenna was also investigated and it was very near to the analytical pattern.

The last example is a microstrip patch antenna, which was taken from [13]. Figure 11 shows that the classic error estimator is once again superior to the residual error estimator.

MULTILEVEL METHODS

In our multilevel methods, the multilevel refers to different orders of $H^P(\mathrm{curl})$ hierarchical basis functions on a single grid. We start from constructing a set of hierarchical vector basis functions with maximum orthogonality [5]. By numbering unknowns from the lowest level to the highest level in $H^P(\mathrm{curl})$, we have the system matrix A_P in the following block structure:

$$A_P = \begin{bmatrix} A_{00} & A_{01} & \Lambda & A_{0p} \\ A_{10} & A_{11} & & \mathrm{M} \\ \mathrm{M} & & \mathrm{O} & \mathrm{M} \\ A_{p0} & \Lambda & \Lambda & A_{pp} \end{bmatrix} \tag{9}$$

Where upper case index letter P stands for all unknowns in $H^P(\mathrm{curl})$, and lower case index letters stand for the additional unknowns at each level in the hierarchy. In multi-level concepts, it is more convenient to rewrite the above matrix in the following two-level recursive form:

$$A_P = \begin{bmatrix} S_{P-1} & A_{P-1,p} \\ A_{p,P-1} & A_{pp} \end{bmatrix} \tag{10}$$

The Schur decomposition of the above matrix takes the following form:

$$A_P = \begin{bmatrix} S_{P-1} & A_{P-1,p} \\ 0 & A_{pp} \end{bmatrix} \begin{bmatrix} I_{P-1} & 0 \\ A_{pp}^{-1} A_{p,P-1} & I_{pp} \end{bmatrix}$$
$$S_{P-1} = A_{P-1} - A_{P-1,p} A_{pp}^{-1} A_{p,P-1} \tag{11}$$

Based on Schur decomposition, we develop our first multi-level preconditioner as follows: S_{P-1} is approximated by $B_{P-1} = A_{P-1}$ and A_{pp} by $B_{pp} = LDM^T$, an incomplete LU decomposition with thresholding, which takes advantage of maximum orthogonality of the basis functions. In the decomposition, L and M stand for strictly lower triangular matrices, D stands for a diagonal matrix and superscript T for transpose. The preconditioner is a multiplicative preconditioner:

$$B_P = \begin{bmatrix} B_{P-1} & A_{P-1,p} \\ 0 & B_{pp} \end{bmatrix} \begin{bmatrix} I_{P-1} & 0 \\ B_{pp}^{-1} A_{p,P-1} & I_{pp} \end{bmatrix} \tag{12}$$

When $A_{P-1,p}$ and $A_{p,P-1}$ are further ignored, we obtain our second multi-level preconditioner, an additive preconditioner:

$$D_P = \begin{bmatrix} B_{P-1} & 0 \\ 0 & B_{pp} \end{bmatrix} \tag{13}$$

Compared with the additive preconditioner, the multiplicative is more attractive. Although it requires additional matrix vector multiplication with respect to the off diagonal blocks, the number of conjugate gradient iterations is significantly less. Furthermore, there is no additional memory requirement because the off diagonal blocks are stored in the system matrix A_P.

Modal analysis shows that matrix A_P has two sets of negative eigenvalues: non-physical ones and physical ones [14]. They correspond respectively to the gradient space and the resonance modes of the physical structure with resonance frequency lower than the prescribed frequency. They cause the convergence problem of conjugate gradient methods without proper preconditioning. Our basis functions so constructed treat the two sets of negative eigenvalues differently: the non-physical ones are represented by the pure gradient vector basis functions and can be easily preconditioned to positive eigenvalues; while the physical ones are represented by lower order vector basis functions and can be preconditioned by complete factorization.

From the above analysis, when the mesh is fine enough, A_{pp} is positive definite and an incomplete LU with thresholding is a good approximation. The complete factorization is only preformed on $B_{P-1} = A_{P-1}$ at the lowest level, i.e., A_0. When the mesh is coarse, the complete factorization must be performed on $B_{P-1} = A_{P-1}$ at a higher level.

To demonstrate the efficiency of MPCG, we have set up a parallel plate waveguide model with cross section 100mm × 60mm. H^1(curl) vector basis functions are used, which results in a two-level block system matrix. The relative residual norm for MPCG is

1.0e-04. We solve the problem with mesh refinement at 5GHz. Figure 1 shows the number of conjugate gradient iterations. It can be seen that the number of CG iterations is almost a constant. In fact, it is slightly reduced with finer mesh. The reason is that H^0(curl) solution improves with mesh refinement, which means a better approximation to those nonphysical negative eigenvalues. The results in Figure 2 show that computational complexity is about *O(n)*, which is what multigrid methods theory has predicted. It should be pointed out the *O(n)* complexity is thanks to the slight decrease of number of conjugate gradient iterations and the cost of decomposition, which includes complete decomposition and incomplete LU decomposition with thresholding, is insignificant in the solution process. As matrix size gets even larger, a higher computational complexity is expected since the cost of decomposition becomes dominant.

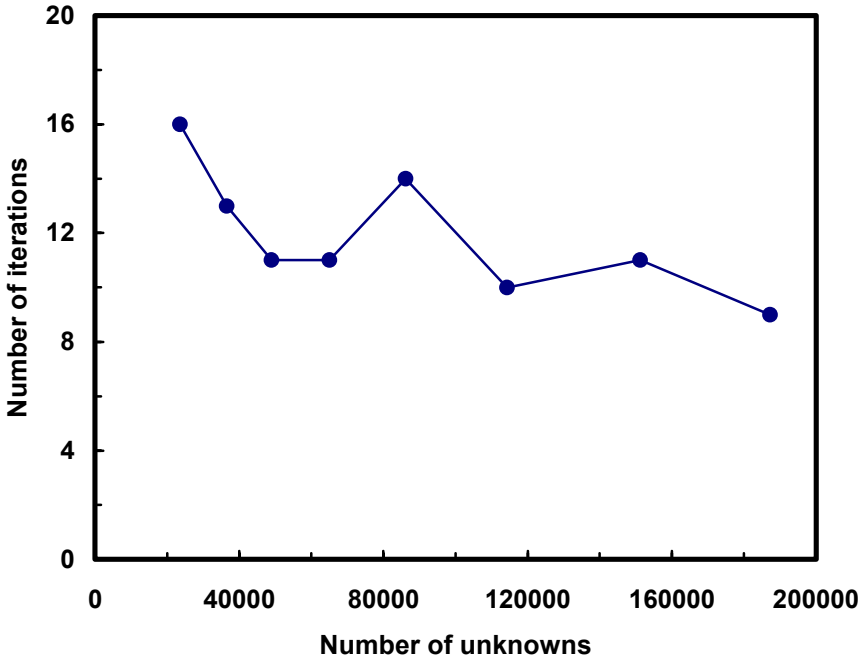

Figure 4 Number of CG iterations

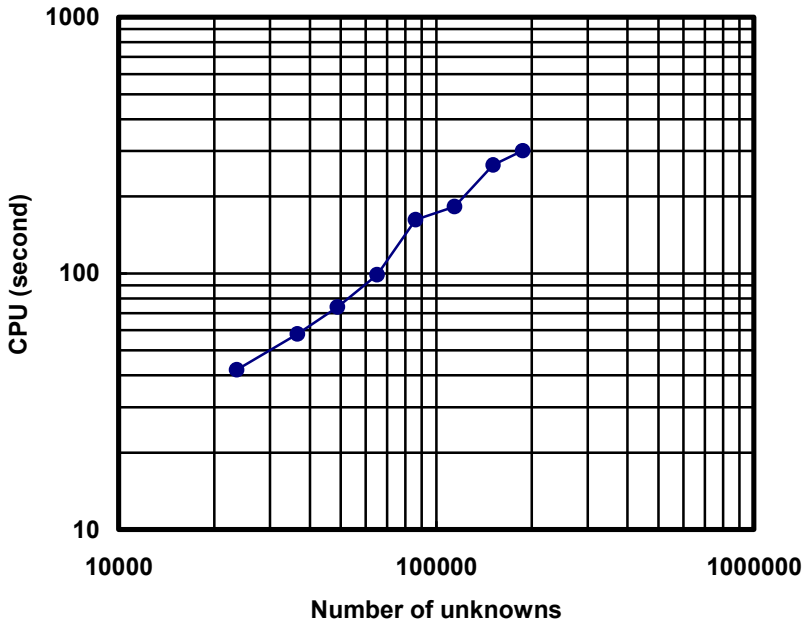

Figure 5 Computational complexity

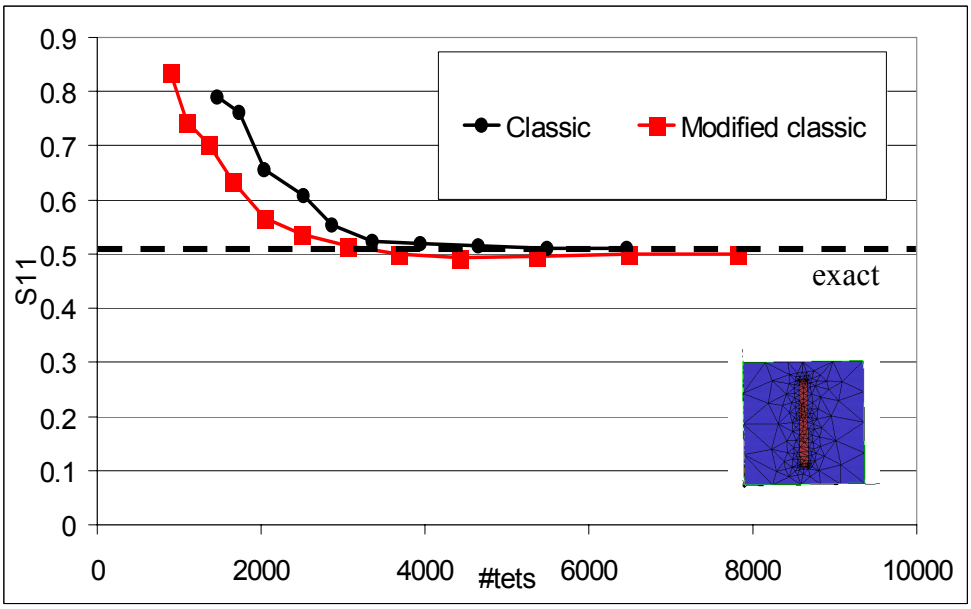

Figure 8: Convergence of the classic and the modified classic error estimator in the case of a slot.

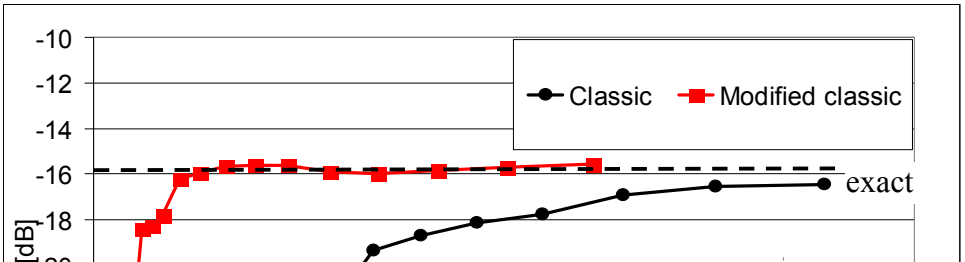

Figure 9: Convergence of the classic and the modified classic error estimator in the case of a low pass filter (LPF).

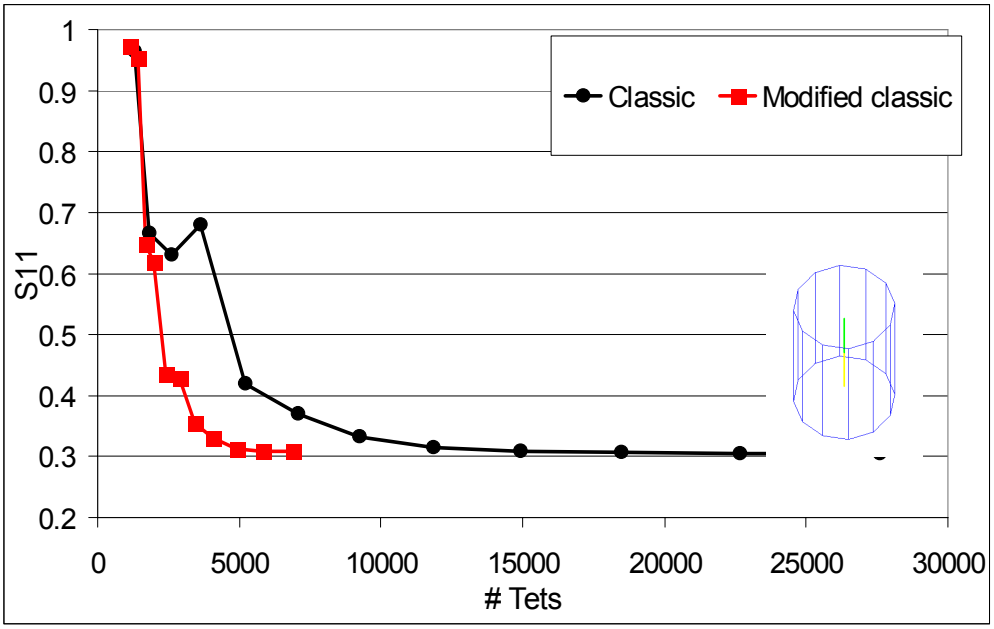

Figure 10: Convergence of the classic and the modified classic error estimator in the case of a half wave length long dipole antenna.

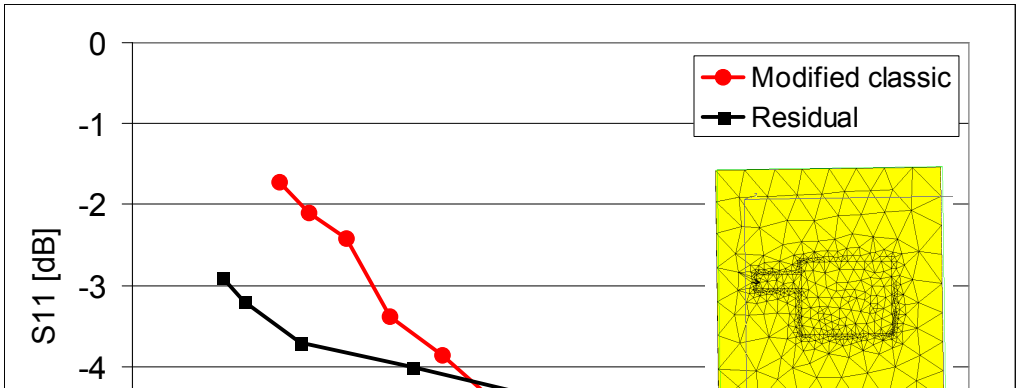

Figure 11: Convergence of the residual and the modified classic error estimator in the case of a patch antenna.

CONCLUSIONS

Adaptive mesh refinement has been used for nearly two decades in electromagnetics to speed the convergence of finite element methods. This technology has two principle elements: unstructured mesh generation and local error estimation. Delaunay tessellation and its variants are commonly used to generate unstructured meshes. Error estimation is generally done by either using residual-based methods or methods based on complementary variational principles. Our experience shows that in most cases, though not all, methods based on complementary variational principles exhibit superior convergence to residual methods.

Matrix solution is made more rapid by using a combination of multifrontal direct solution and iterative multilevel solutions. Multifrontal methods allow million unknown problems to be solved in a few minutes on a PC while iterative multilevel solvers provide linear performance with even larger problems.

While the capacity and performance of computers are continually growing, an even more important factor in increasing the size of problems that can be solved has been advances in simulation algorithms. We have found through twelve years of experience with HFSS that both adaptive mesh generation and the multilevel solution methods accelerate finite element solutions dramatically.

REFERENCES

[1] *HFSS User's Guide,* Hewlett-Packard Company, October 1990.

[2] Z. J. Cendes, D. N. Shenton and H. Shahnasser, "Magnetic Field Computation Using Delaunay Triangulation and Complementary Finite Element Methods", *IEEE Transactions on Magnetics,* Vol. 19, No. 6, pp. 2551-2554, November 1983.

[3] D. N. Shenton and Z. J. Cendes, "MAX – An Expert System for Automatic Adaptive Magnetics Modeling", *IEEE Magnetics,* Vol. 22, pp. 805-807, 1986.
[4] J. Lee, D. K. Sun and Z. J. Cendes, "Full-Wave Analysis of Dielectric Waveguides using Tangential Vector Finite Elements", *IEEE Transactions on Microwave Theory and Techniques,* Vol. 39, No. 8, pp. 1262-1271, 1991.
[5] D. K. Sun, J. Lee and Z. J. Cendes, "Construction of Nearly Orthogonal Nedelec Bases for Rapid Convergence with Multilevel Preconditioned Solvers", *SIAM Journal on Scientific Computing,* Vol. 23, No. 4, pp. 1053-1076, 2002.
[6] R. E. Bank and A. H. Sherman, "An Adaptive, Multi-level Method for Elliptical Problems", Computing, Vol. 26, pp. 91-105, 1981.
[7] Z. J. Cendes, "Vector finite elements for electromagnetic field computation", *IEEE Transaction on Magnetics*, Vol. 27, No. 5, pp. 3958-3966, September 1991.
[8] J. F. Lee, D. K. Sun, and Z. J. Cendes, "Tangential vector finite elements for electromagnetic field computation", *IEEE Transactiosn on Magnetics*, Vol. 27, No. 5, pp. 4032-4035, September 1991.
[9] D. K. Sun, Z. Cendes and J.F. Lee, "Adaptive Mesh Refinement, h-Version, for Solving Multiport Microwave Devices in Three Dimensions", *IEEE Transactions on Magnetics,* Vol. 36, pp. 1596-1599, July, 2000.
[10] A. M. Arthurs, *Complementary Variational Principles*, Clarendon Press, Oxford, 1980.
[11] I. Bardi and O. Biro, "An Efficient Finite-Element Formulation Without Spurious Modes for Anisotropic Waveguides", *IEEE Transactions on Microwave Theory and Techniques,* Vol.. 39, pp. 1133-1139, July, 1991.
[12] I. Kondor, "Duality-based error estimator and mesh adaptivity in CFD," Diploma Course Report, von Karman Institute for Fluid Dynamics, Rhode Saint Genese, Belgium, June 2000.
[13] J. Van Bladel, "Singular Electromagnetic Field and Sources" Claredon Press – Oxford, 1991.
[14] R. Dyczij-Edlinger and O. Biro, "A Joint Vector and Scalar Potential Formulation for Driven High Frequency Problems using Hybrid Edge and Nodal Elements", *IEEE Transactions on Microwave Theory and Techniques,* Vol. 44, pp. 15-23, 1996.